

Optical Navigation Analyses for Hera Proximity Operations: Early Characterization Phase and Detailed Characterization Phase

Ignacio Acedo⁽¹⁾, Pablo Muñoz⁽²⁾

⁽¹⁾GMV, located at ESOC
Darmstadt, Germany
<firstname>.<lastname>@ext.esa.int:

⁽²⁾ESA
Darmstadt Germany
<firstname>.<lastname>@esa.int:

Abstract – The Hera mission, scheduled for launch in October 2024, targets Proximity Operations around the Didymos system to characterise the asteroid system and with a special focus on the effects of DART impact. As part of the preparations for this mission, a set of tools for optical navigation analysis has been developed to assist with the preparations of trajectories for the Proximity Operations (PO) phase around the asteroid. The first part of this paper describes these tools, with a focus on the optical observable modelling for both centering and landmark observables. This is then followed by the presentation of navigation analysis results for the Early Characterization Phase and Detailed Characterization Phase of the Hera mission, as they show the planned use of these two types of observations and give an insight on their performance and limitations.

I. INTRODUCTION

The Hera mission, scheduled to launch in October 2024, is the European component of the AIDA (Asteroid Impact and Deflection Assessment) collaboration between ESA and NASA [1], [2]. AIDA consists of an asteroid impact test on the secondary of the binary asteroid system Didymos, called Dimorphos. Following the successful impact of DART with Dimorphos on the 26th of September of 2022, the Hera mission is tasked with carrying out a detailed characterization of both asteroids in the system and with the study of the morphological and dynamical effects of the impact in Dimorphos.

The Hera spacecraft and its mission are, in many ways, inspired by the Rosetta mission. This ESA mission stayed in the proximity of comet 67P/Churyumov-Gerasimenko starting during the summer of 2014 and ending its mission in September of 2016. The manoeuvring of the Rosetta spacecraft relied on the use of optical observations [3] of the comet to refine the relative orbit determination between it and the spacecraft [4]. The use of optical observables is commonplace for small body rendezvous missions, with other past examples being NEAR [5], Hayabusa [6], Hayabusa II [7], Dawn and OSIRIS-REX [8]. Optical

observations provide valuable information on the relative state between the spacecraft and the observed body. In the case of Hera, they will also be critical to achieve the mission objective of a thorough characterization of the system dynamics post DART impact.

II. METHODOLOGY, MODELS AND ASSUMPTIONS

A. Analysis methodology

The navigation analyses carried out are comprised of two distinct and separate parts. The first is the Knowledge Analysis, in which a simulation of the orbit determination (OD) processes is performed. By knowledge here we refer to the accuracy of the estimation performed by the OD. This simulation serves to estimate the knowledge available for each commanding cycle. Its results are then used for the second part of the analysis, the dispersion or guidance simulation. It consists of the simulation of the evolution of dispersion from the spacecraft nominal trajectory under a given set of perturbations, including the effects of OD uncertainty and manoeuvre execution error. These two analyses are run iteratively until the sizes of the commanded manoeuvres have converged.

Both analyses are conducted using tools developed for this purpose on top of GODOT, ESOC Flight Dynamics' software for Generic Orbit Determination and Optimization of Trajectories [9].

The knowledge and dispersion analyses rely on linearized dynamics: the deviations in spacecraft states are mapped in time using the State Transition Matrix (STM), which is precomputed for the assumed reference trajectory. For this approach to be valid, it is necessary that the mapped deviations are sufficiently small so that there is not a high degree of disagreement between the linearized dynamics and the actual, non-linear dynamics.

The Knowledge analysis is itself a covariance analysis, performed using a Square Root Information Filter (SRIF). Parameters can be estimated (solve-for) or considered. The knowledge covariance of the estimated parameters is improved by incorporating observations. On the other hand, the considered parameters uncertainty cannot be reduced, and thus, these increase the resulting covariance of the solve-for parameters. At

last, the resulting covariance can be mapped to other epochs and/or state representations.

For each OD arc, all observations between a fixed initial epoch and the data cut-off of each manoeuvre are included.

For the dispersion analysis, a 5000 sample Monte Carlo simulation of the linearized dynamics around the reference trajectory of Hera is performed. For each sample being propagated, an initial dispersion of the relative state between Hera and Dimorphos is propagated between the simulated manoeuvres. Then, in each manoeuvre, a random estimation error based on the Knowledge Analysis is drawn. This is used to calculate an estimated dispersion from the reference trajectory, which in turn serves to calculate the manoeuvre correction to be applied on top of the nominal manoeuvre to recover the spacecraft position at the following epoch. Apart from this commanded correction, a random manoeuvre execution error is sample to calculate the executed manoeuvre. This dispersed post manoeuvre state is then propagated on to the next manoeuvre until the end of the simulation.

As mentioned before, these two analyses are run in an iterative sequence, checking for convergence on the simulated manoeuvre sizes. The convergence threshold is set at 2 % of the manoeuvre size.

B. Observation models and assumptions

Both radiometric and optical observations are to be used for navigation operations around the Didymos system. The radiometric observations include Two-Way Range and Range-Rate observations. While Hera has the capability necessary for Delta-DOR measurements, the availability of optical observations and the need for extra processing of such measurements for correlation of the signals discourage their use through Proximity Operations. Assumed performances for Two Way Range and Two-Way Range-Rate observables are listed in Table 1.

Table 1: Radiometric observables performance assumptions

	Value (1- σ)	Treatment
2-way Range noise	2 m	Obs. noise
2-way Range bias	10 m	Consider
2-way Doppler noise	0.1 mm/s	Obs. noise

Since Optical observables are the focus of this article, we will delve deeper into their modelling and setup. Hera will carry two Optical Asteroid Framing Camera's (AFC) which will be located in its instrument deck. These cameras have been assumed to have a 5.5x5.5deg Field of View (FoV) and 1024x1024 pixels of resolution. While the final camera characteristics are slightly different, the results remain relevant as this would have negligible effect on the navigation analysis results. When in Proximity Operations, both Didymos

and Dimorphos will be resolved on the on-board camera, with an apparent size for Didymos between 1.5 and 4.5 degrees for the distances covered by the spacecraft through the first parts of Proximity Operations. The pixel size at 30 km is 2.8 m and at 10 km is 0.9 m. The images used for navigation will be processed for two different kinds of observations. Firstly, centering-style algorithms (such as Lambertian Sphere fits, or centroiding) will be used to try and estimate the position of the asteroid centre of mass from the observed illuminated part of it. Algorithms of this kind will be used already through the rendezvous phase [10] and are to be used in this first phase of the Proximity Operations as they do not require a detailed model of the asteroids for their functioning. The main drawback of these algorithms is that they only provide plane of sky observability of the relative position, and thus requires the reliance on radiometric measurement to reconstruct the relative state between asteroid and spacecraft. Since Didymos is a binary system, measurements of this kind will be generated for both asteroids when they both appear in the FoV of the camera and thus, when combined, they can provide a parallax measurement which gives information on the distance to the system. For example, when the two asteroids are observed from 30 km away with an uncertainty of 100 m [1-sigma] on the relative measurement and a separation between the two of 1 km, the parallax may get information on the distance to the system of the order of 2 km [1-sigma], which is insufficient to achieve performant navigation.

The second kind of measurements to be generated are landmark/mapplets optical observations. By a landmark model we refer to a model in which features on the asteroid surface are identified and catalogued in a model to then, for each new navigation image, identify the observable features and locate them in the image. With this, a line of sight measurement is produced for each visible landmark in the image. The reader can find more details of their implementation for Rosetta in [3]

Within our analysis modelling suite, both centroiding and landmark models share a similar framework used to model optical observation. The Optical observation class, which each specific model derives its own implementation from, includes a Camera model and a list of target points. For each scheduled observation, the camera model assesses the observability of each target. Also, different target models may also provide additional checks for observability, as it is the case of the landmarks model. For each observable target, the angular distance to the camera boresight in the two directions of the plane of camera is calculated. Bias parameters may be added for the camera pointing direction uncertainty, representing systematic errors on the determination of the camera's boresight with respect to the inertial frame. Also, target models can implement their own biases which will be accounted into the observation generation. For centroiding targets, the bias is added as a fraction of the asteroid size and represent a

constant offset between the centre of the asteroid shape pointed to by centroiding algorithms and the asteroid centre of mass. Along with this, an equivalent process is followed to generate the measurement weights, the inverse of the measurement noise, to be used in the filtering of observations. Here as well, a combination of a generic observation noise on the camera side on one hand and on the target model side on the other is possible. On the camera side the noise represents the instrument noise, usually at pixel level, while on the target side this represents an algorithmic noise. On the centroiding algorithm, a centroiding noise is defined as a percentage of the target body size. No extra algorithmic noise is added to the landmark observables, as the pixel level noise is the performance assumed for the maplet correlation.

The goal of this modelling framework is to give the analyst flexibility when setting up optical models, allowing the use of composition to generate complex models which combine different kinds of observation targets or to define their own target models as required by each analysis' specific needs.

For navigation analysis, the FoV of the camera is assumed to be circular with a half-cone angle of 2.75 degrees around the boresight. Errors and biases for the camera observable are applied in both directions of the FoV unless stated otherwise. A consider bias of 10 mdeg [1-sigma] is assumed to account for errors on the estimation of the camera pointing direction from the on-board attitude monitoring and a 1 pixel [1-sigma] assumption on baseline instrument noise is taken. Centroiding observations both of Didymos and Dimorphos are planned for navigation of the Early Characterization Phase, with an assumption of centroiding noise of 10% [1-sigma] of each asteroid's diameter. Along with this, a 10 % [1-sigma] consider bias on these images is assumed plane. These biases are assumed to be independent for Didymos and Dimorphos. For the Detailed Characterization Phase analyses, a landmark model for Didymos is used. This landmark model takes 50 random points out of the Didymos shape model taken so that each of them lies at least 10 degrees away from other landmarks in the model. The distribution of landmarks can be seen in Fig. 1.

The landmark model used is based on models used for Rosetta Orbit Determination activities around the comet [4] and includes the option of defining a model bias (\mathbf{b}) with respect to the asteroid centre of mass \mathbf{x}_{CM} as well as a scaling factor (s) for the whole model, as seen in (1):

$$\mathbf{x}_{landmark_i} = \mathbf{x}_{CM} + \mathbf{b} + s * \mathbf{x}_{i_i} \quad (1)$$

This model has been validated using legacy Flight Dynamics Software developed for Rosetta's comet operations. Within the context of the navigation analysis, the bias and scaling parameters are not used.

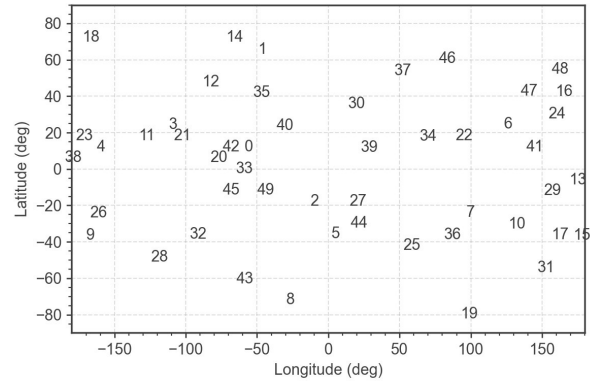


Fig. 1: Didymos Landmarks distribution

C. Operations Scheduling and Observational Constraints

Since Hera has a non-steerable High Gain Antenna (HGA), it needs to acquire an Earth Pointing attitude for Ground Communications. As such, the operational timeline through PO is split between Asteroid Pointing and Earth Pointing Periods. The ground communications slot is preferably located through the European night, favouring the use of Malargüe as main station. 8 hours a day are assumed to be allocated to ground communications, with 13 hours destined to asteroid observations and the rest allocated to slews and used as margin. Radiometric observations are taken through the Earth Pointing period, with a minimum elevation of 15 degrees over the station's horizon assumed for radiometric observables. Two Way Range observables are produced at a cadence of once every hour while Two Way Range-Rate observables are produced every 10 minutes.

Through the Asteroid Pointing Periods, the spacecraft is assumed to be facing its instrument panel towards the Didymos asteroid, including its navigation camera. Five images per day are assumed to be taken, equally spaced through this period. For centroiding measurements, Didymos is assumed to be visible in all images, while Dimorphos is only accounted for in case that: a) there is no partial occultation between the two bodies, and b) the angular distance between the Didymos centre and the Dimorphos outer lobe as seen from the spacecraft is smaller than half the width of the FoV. For this purpose, Dimorphos is assumed to have a spherical shape with a radius of 90 m.

For landmark observations, observability conditions are checked individually for each landmark. The landmark is to be sufficiently illuminated by the Sun, with a minimum Sun elevation over the local horizon of 20 deg and not be in Dimorphos' shadow. Also, a minimum spacecraft elevation over the local horizon of 20 degrees is demanded. In both cases, the asteroid is assumed to be spherical for the purposes of defining the local horizon plane. Finally, the landmark must not be occulted by Dimorphos.

Regarding commanding scheduling, a 3-4 day pattern is synchronised to the working week, with commanded periods starting in the early morning of Wednesday (I) and Saturday (II). Each commanded period starts with a manoeuvre. A two-day turn around time for the ground commanding cycle is assumed and thus, the latest observations for OD in each cycle are downlinked through the Sunday night for period I and on Wednesday night for period II. Then, commands are uplinked through the pass in Tuesday evening for period I and in Friday evening for period II. This schedule leads to one day of observations for cycle I, following its manoeuvre before data cut off (DCO), while two days of observations are available through cycle II.

D. Dynamics Modelling and A-priori uncertainties

The spacecraft dynamics model used includes gravitational forces and solar radiation pressure on the spacecraft. As shown in Fig. 2, the two main dynamic contributions around Didymos are Didymos gravitational pull and the solar radiation pressure. In any case, to maintain a coherent model, Hera is propagated accounting with gravitational pull from the Sun, all of the planets and the two asteroids on the system. [11] gives already some estimates on Didymos and Dimorphos' mass, however, the further expansions of the gravitational fields can only be speculated upon with the information available at this moment. The values used for this analysis are obtained by assuming a total mass of 6.05×10^{11} kg, and using the ratio of mean diameters and assumed densities for distributing the system mass between the two. For Didymos the assumed density is 2950 kg/m^3 and for Dimorphos the lower bound of 2000 kg/m^3 from the 2000 – 3000 kg range is chosen.

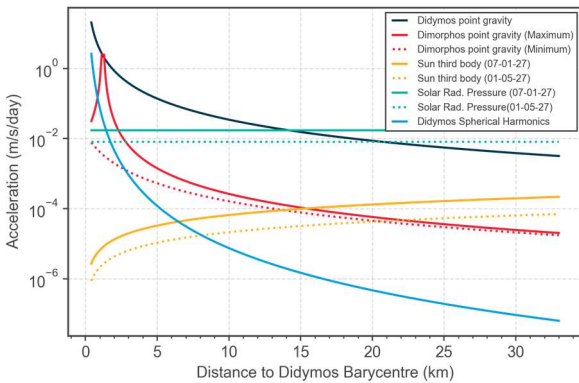


Fig. 2: Dynamical Environment around the Didymos system distribution

Table 2: Asteroid GMs assumptions

Body	GM
Unit:	km^3/s^2
Didymos	4.01×10^{-8}
Dimorphos	2.36×10^{-8}

A-priori knowledge uncertainties and dispersions in these values are phase dependent.

For Didymos, a J_2 value is calculated assuming constant density and an ellipsoid shape, which allows the use of the following (2), as taken from [4].

$$C_{20} = -J_2 = \frac{I_{xx} + I_{yy} - 2I_{zz}}{2M \times r_{ref}^2} \quad (2)$$

Within the simulations expansions up to order 4 and degree 4 for Didymos and order 2, degree 2 for Dimorphos of nominal value 0 are included to introduce uncertainty on the higher order parameters. The a-priori uncertainty in this value is derived by choosing upper bounds for each degree and order pair from a calculated expansion on a radar model with constant density for Didymos 4x4 field, which was an evolution by the DART team pre-impact of the radar model presented in [11]. For Dimorphos, a similar process using an ellipsoid was carried out.

For the solar radiation pressure (SRP), a flat plane model is used to propagate Hera, with the following characteristics. For Knowledge Analysis a 1% [1-sigma] consider uncertainty on the nominal Cr is used while for dispersion analysis, a 1% [1-sigma] bias is generated for the whole simulation.

Finally, Non Gravitational Accelerations are also used for propagating Hera to account for other uncertain disturbances, such as non-radial SRP components and Wheel Off Loadings. For knowledge analyses these are represented as solve-for Exponentially Correlated Random Variables with autocorrelation time of 1-day in each of the three cartesian directions. The a-priori uncertainty is $1e-11 \text{ km/s}^2$ [1-sigma] which is meant to account for a wheel off loading frequency of once every three days. Along with this a bias in all directions of $1e-12 \text{ km/s}^2$ [1-sigma] is treated as a consider sigma.

Following the impact of DART with the Didymos system, observations of the system have confirmed a significant change in orbital period. However, the exact details of the orbit remain unknown. For this purpose, a nominal circular orbit is assumed. This has the advantage of allowing a parameterization of the asteroid orbit which remains linear in its variations with respect to the known parameters defining the satellite orbit. This is key to ensure the validity of the linear dynamics model used for this analysis. The model assumes a nominal circular and equatorial orbit, and as such the orbit can be modelled as a Keplerian orbit with a modified equivalent gravitational parameter with accounts for the centripetal acceleration from Didymos J_2 component of its gravitational model. Since the period is a well-known parameter, the initial orbital state is defined as a function of the gravitational parameters, the observed period, null eccentricity and inclination vectors and an initial true longitude ($\lambda = \omega + \Omega + \nu$). This is done by equalizing the centripetal force for a circular orbit with the experienced forces, obtaining the following expression:

$$\dot{\lambda}^2 r = \frac{\mu_D \left(1 + \frac{3}{2} J_2 \left(\frac{r_{ref}}{r}\right)^2\right) + \mu_d}{r^2} \quad (2)$$

Where $\dot{\lambda}$ is the true longitude rate (the true longitude being the addition of the longitude of periapsis and the true anomaly, r is the orbital radius, μ_D Didymos gravitational parameter, μ_d the Dimorphos gravitational parameter and J_2 and r_{ref} are those of Didymos spherical harmonics model. The values used are listed in Table 3:

Table 3: Relative Orbit Parameters @ 10-02-2027 00:00:00.0 TDB

Parameter	Value	Unit
True Longitude Period	11.3685	hours
Initial True Longitude	45	deg
Orbital Radius	1.202	km

These parameters are set at 00:00 UTC, on the 2nd of February of 2027, around the middle of nominal proximity operations. The phasing chosen for this point is arbitrary and it most likely not to match the system's actual phasing. For knowledge and dispersion analysis a-priori uncertainties are dependent on the phase also for these values. The initial state of the asteroid barycentre at this epoch is fetched from the solution available in the JPL Horizons database as of the 6th of July 2023. The translational system dynamics simulation takes into account the gravitational point gravity from the planets and the Sun, the point gravity and J2 component from Didymos and the Dimorphos point gravity. The propagation is not coupled with the rotational dynamics of the asteroids, which is acknowledged to have a potential effect on the translational dynamics due to energy exchanges between the asteroids. Also, regarding the rotational dynamics, a pure rotation around the major inertia axes without external torques is simulated for Didymos, with a period of 2.26 hours, while for Dimorphos a tidal lock rotational state is assumed. It must be noted that following the DART impact, a pure tidal lock is not likely, and a small libration around the tidal lock state is the more likely behaviour, although it is not discarded that the asteroid may have been spun into a chaotic rotational state (see more in [12]). Despite these simplifications in translational and rotational dynamics, the navigation of Hera should not be disturbed by variations in these (due to the high distance it does not note an effect of the spherical harmonics field of Dimorphos). The chaotic Dimorphos rotational state make the use of landmark navigation on it challenging, and thus as a conservative assumption no landmark observations on Dimorphos are used in these simulations.

E. Manoeuvre Guidance and modelling

For the navigation analysis, a simple position correction

scheme is chosen as the guidance law, where, for each manoeuvre, the position error at the next manoeuvre is corrected. Hera has the capability to execute manoeuvres in two manners. The first uses its main Orbit Control Thrusters (OCT), which requires a dedicated attitude to be adopted through the manoeuvre, while the second uses the Reaction Control Thrusters (RCT) to achieve an effective delta V through combined firing. Conservative manoeuvre execution error assumptions are taken for each thrusting mode.

Table 4: Three sigma error assumptions for Hera thrusting modes.

Thruster	Magnitude Error	Direction Error
Unit:	%	deg
OCT	5	2.5
RCT	6	6

For modelling manoeuvre errors in the context of the guidance analysis, the commanded manoeuvre is taken, and a magnitude and direction errors are sampled from respective normal distributions. The direction error is applied in a direction around the nominal manoeuvre vector randomly selected from a uniform distribution covering the whole rotation around such nominal manoeuvre.

F. Reference Frames

Through the document, several reference frames will be used to describe the trajectory and products of the navigation analysis. These are the following:

- **Sun Fixed Didymos Equatorial:** This reference frame is Didymos centred and is used for depicting Hera's trajectory around the system. The X axis points from Didymos to the Sun, the Y axis is inscribed in Didymos equatorial plane and the Z axis points towards the northern hemisphere of Didymos. The Y axis direction is chosen so as to define a right-handed triad.
- **Centre-Orbiter RAC:** A Radial, Along-Track, Cross-Track triad described by the relative motion between a central body and an orbiter. In practice, Didymos-Hera RAC and Dimorphos-Hera RAC are used in this paper.

III. GETTING READY FOR THE ACTION: EARLY CHARACTERIZATION PHASE NAVIGATION (ECP)

A. ECP Trajectory and Operational Characteristics

Once Hera reaches the vicinity of the Didymos system, a first, the Early Characterization Phase (ECP) is tackled. This phase takes 6 weeks, spanning from the 2nd of December 2026 to the 13th of January 2027 and follow the rendezvous and descent to asteroid proximity undertaken through the months of October and November. This phase is to be used by the ground teams

to perform an initial characterization of the system at close distance (as the descent towards the system in the previous phase will already a very early characterization of the system).

The spacecraft through this phase describes a rectangular loop in the Sun Fixed Didymos Equatorial frame (see Fig. 3), with manoeuvres at a distance to Didymos of 30 km and phase angles of 47 degrees, as shown in Fig. 4.

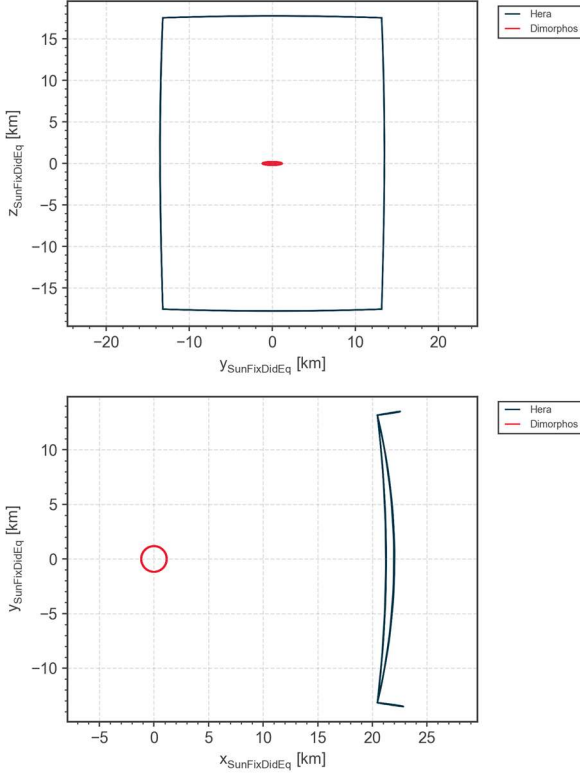


Fig. 3: ECP Geometry around Didymos in Sun Fixed Didymos Equatorial frame. Top: Y-Z projection. Bottom: X-Y projection

The selection of these parameters followed a study of previously proposed trajectory, as this is the smaller phase angle which allows for executing manoeuvres without dogleg splits due to infringement of the target safety margin over the escape velocity at the osculating pericentre of 0.4. This parameter is obtained by dividing the instantaneous velocity with respect to the system barycentre by the instantaneous escape velocity. While higher phase angles would have been preferred as they would allow more diverse observation conditions for the characterization of the system, navigation analyses on higher phase angle trajectories showed high prediction errors of the spacecraft trajectory due to higher manoeuvre sizes and thus higher manoeuvre errors. These then translated into high pointing errors when following the ground commanded attitude profile which led to a too early loss of the asteroid system from the FoV, compromising navigation performances and the characterization goal.

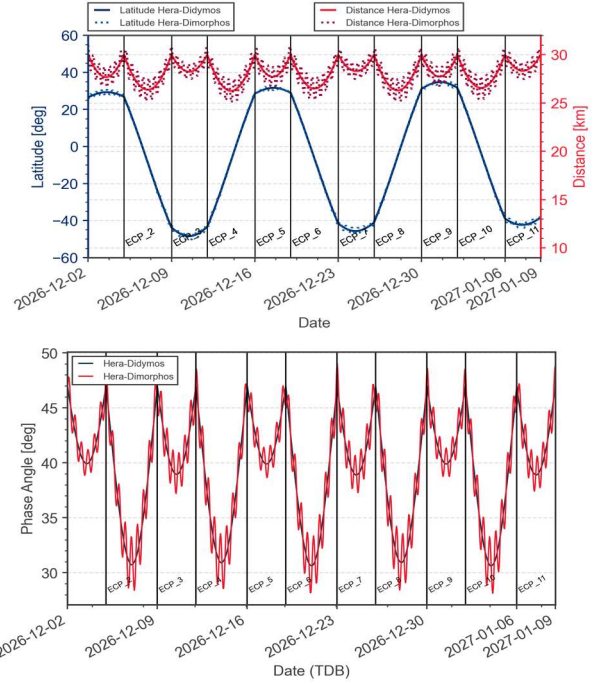


Fig. 4: ECP Geometrical Parameters. Top: Distance and Latitude. Bottom: Phase Angle

B. Phase specific navigation assumptions

Through this phase the ground teams will also have the opportunity of exercising and commissioning the spacecraft on-board autonomous attitude guidance capabilities. From a navigation point of view, the phase entails two main limitations on the capabilities of the spacecraft.

1 – While a detailed model of the system is generated, optical navigation must rely on centering style observables to estimate its state with respect to the system and to determine the system's state.

2 – Since autonomous attitude guidance is not yet available at this stage, the spacecraft must rely on ground commanded attitude profiles.

The use of OCT thruster is baselined for this phase. The knowledge analysis accounts for observations also in the prior two arcs before the start of ECP. The a-priori knowledge for Hera and the Didymos Barycentre state is derived from previous analysis of the rendezvous phase [10] and is listed in Table 5, along with values for the asteroid gravitational parameters and the initial state of the secondary's orbit. The values for parameters are given large a-priori to show how performant is the filter in lowering the uncertainty without prior knowledge of the parameters. Table 6 shows the dispersion assumptions.

Table 5: ECP Specific Solve-For Parameter Assumptions [1- σ]

Parameter	Value	Unit	Notes
Hera Position	10	km	Spherical
Hera Velocity	1	mm/s	Spherical
Didymos Barycentre Position	10	km	Spherical
Didymos Barycentre Velocity	1	m	Spherical
True Longitude Period	100	s	
Didymos GM	100	%	
Dimorphos GM	200	%	
e_x, e_y	1.0	-	
i_x, i_y	1.0	-	
λ_0	180	deg	

Table 6: ECP Specific Navigation Analysis Dispersion Assumptions [1- σ]

Parameter	Value	Unit	Notes
Didymos-Hera Position	10	km	Spherical
Didymos-Hera Velocity	1	mm/s	Spherical
True Longitude Period	1	s	
Didymos GM	16	%	
Dimorphos GM	100	%	
e_x, e_y	0.03		
i_x, i_y	0.1151	-	Equivalent to 40 deg [3-sigma] in pole solution
λ_0	10	deg	

C. Navigation Analysis Results

Fig. 5 shows the evolution of instantaneous position knowledge between Didymos and Hera through the ECP phase. By instantaneous knowledge we refer to the knowledge of the spacecraft state with observations up to the plotted date minus the 2 days turn-around time used for undertaking the ground operations cycle. This thus serves as an indication of the effect of each observation pass after the preparation of a flight dynamics cycle following such observation. At the time of manoeuvres, it represents the available knowledge for prediction of the state at manoeuvre time used for commanding it.

The position knowledge at manoeuvre times varies significantly between manoeuvres, with some manoeuvres where the uncertainty at manoeuvre times ranges between 250 and 600 m [1- σ]. It can be observed that the variation follows a cycle each 4 manoeuvres, as the spacecraft follows its rectangular pattern. For example, looking at the middle rectangle from ECP 4 to ECP 8, in the first arc a performant estimation is achieved and that through the next two arcs the uncertainty in the radial direction keeps increasing and even through the longer 4-day arc between ECP 6 and ECP 7 there seems to be no good observability of the radial direction. This can be explained by the evolution

of the Earth-Asteroid-Spacecraft angle shown in Fig. 6. When this angle is close to 90 degrees, the direction to the Earth is perpendicular to the line-of-sight to the system and, as such, the radiometric measurements do not provide observability of the radial direction. On the contrary, when this angle is high, the observability of the radial direction is improved.

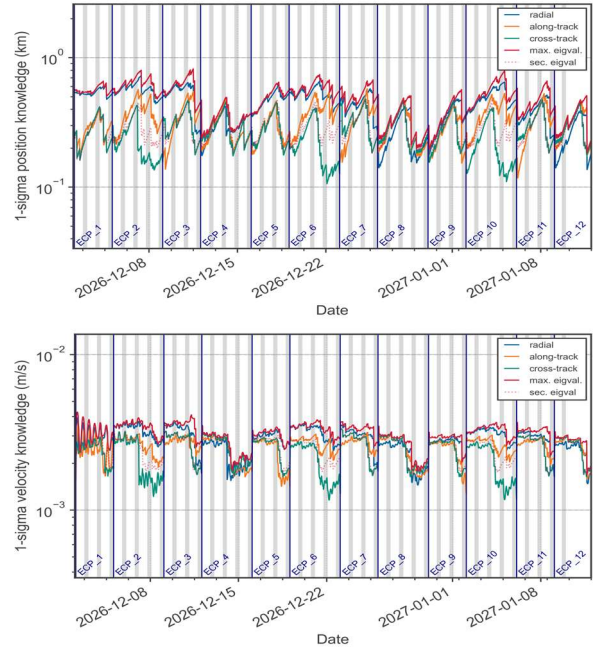


Fig. 5: [1-sigma] ECP Knowledge Evolution. Vertical blue lines signal manoeuvre epochs and grey lines represent radiometric passes. Top: Position. Bottom: Velocity

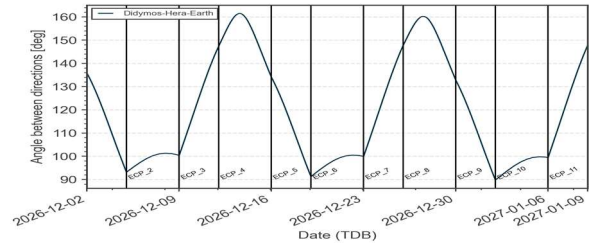


Fig. 6: Didymos - Hera - Earth angle through ECP

The knowledge analysis also allows the study of the evolution of the estimation of the asteroids' orbits and its parameters. Through this phase, some observability of the asteroids' GMs is predicted, with the values going down to 1% [1-sigma] for Didymos, Dimorphos values seem to go down to 60% [1-sigma], but this is still not enough to determine the actual value (see Fig. 7). As it can be expected, no observability of the spherical harmonics field of Didymos nor Dimorphos is possible in this phase. The J2 effect of Didymos on Dimorphos is indistinguishable from the Didymos GM, and thus, once the GM uncertainty of Didymos drops to the level where the uncertainty of the gravitational pull it exerts on Didymos is the same as the effect of the J2, the

uncertainty on both values becomes anticorrelated and it is not possible to reduce it until independent observations of Didymos GM are achieved later in the mission. The relative motion between the two bodies is estimated to a position uncertainty in the along-track direction of 10 m [1-sigma] by the end of the phase, while the other two components of the relative position are estimated down to [1-sigma] uncertainties of 6 m for the radial and of 2.6 m for the cross-track component. This translates into the evolution of the knowledge of the orbital parameters through the phase shown in Fig. 8. The orbital plane is determined down to below 0.1 degrees [1-sigma] and the eccentricity vector is estimated to a spherical uncertainty of 0.04 [1-sigma]. A worse estimation is that of the orbital motion. The initial true longitude is determined down to a level of 0.3 degrees [1-sigma] and the true longitude period is estimated down to 5 seconds [1-sigma] which is not yet better than estimates based on radar observations following the DART impact.

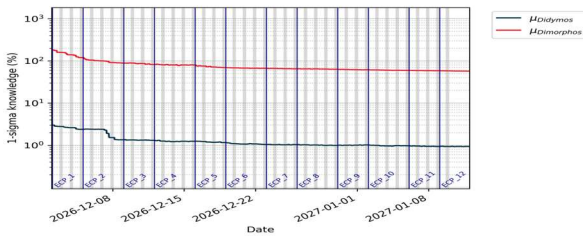


Fig. 7: [1-sigma] ECP Didymos Gravitational Parameters Knowledge Evolution.

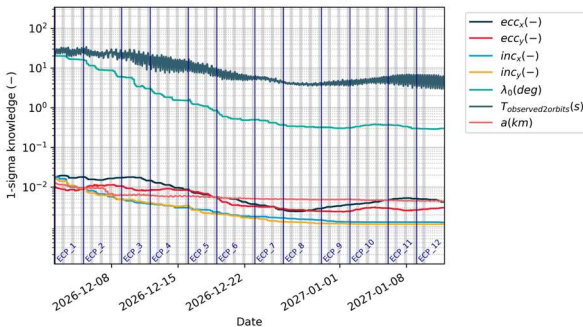


Fig. 8: [1-sigma] ECP System Orbital parameters knowledge. Period uncertainty is given as observation over the last two revolutions.

The position dispersion evolution for this phase oscillates between [1-sigma] values of 2 km at manoeuvre times after poor observability periods (see ECP 7) and 1.1 km for well-behaved arcs once the inflated a priori dispersion converges. This holds well below 10% [1-sigma] levels and thus there is no relevant risk of asteroid impact. The guidance simulation also allows the estimation of a dispersion at 99 percentile of 11.5 cm/s, which sits around 10 % of the nominal allocated delta-v for this phase. A more pressing issue through the ECP is the effect of trajectory prediction errors in the pointing error of commanded attitude profiles. The nominal attitude through asteroid pointing

periods is with the instrument panel pointing towards Didymos, however, the FoV of the AFC is 5.5 degrees wide, which accounts for an image coverage of 2.88 km at 30 km distance. This means that, given that for centroiding it is necessary to have an image of the full body, the imaging strategy is only robust to disturbances under 1 km. In practice, this limitation is overcome by commanding a mosaic of images around the predicted pointing attitude with some overlap between them. A 2x2 mosaic is thus baselined for this phase. To validate this approach, a pointing error simulation based on knowledge covariance analysis. The analysis is set up to account for observations up to the arcs data cut off (two days prior to the start of the arc) to compute a prediction knowledge profile through the whole arc. In two hour intervals, random prediction errors are generated (10 000 samples per data point) and with them the angle between the outer limb of each asteroid and the predicted centre of Didymos is computed. These computations are used to derive timelines for different percentiles and statistics on the percentage of samples within the FoV. The evolution of the 68th and 99th percentile for Didymos is given in Fig. 9. It can be appreciated that for some arcs in the sequence, the 99th percentile goes over the 1 FoV line at 5.5 degrees before Optical DCO, which is the time of the last image to be accounted for the following commanding cycle.

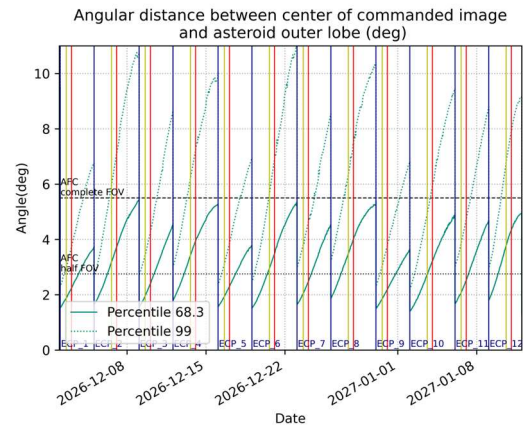


Fig. 9: Evolution of angular distance between Hera AFC boresight and Didymos outer lobe through ECP

This means that there is a plausible chance that some cases would lose images before DCO. For this purpose, a sensitivity analysis was performed in which the observations following the 99th percentile overtaking the 1-FoV mark are dropped. corresponds to such case. This case would see a somehow degraded navigation, where position dispersions increase by a factor between 10 and 20 %. The characterization of the system is degraded. The uncertainty on the estimation of Didymos GM increases by a similar factor of 20% while Dimorphos increases by 60%. The system orbital characterization is not severely degraded. Along with this, this plot also serves to identify candidate arcs for autonomous attitude

guidance commissioning. For this purpose, the requirement is to have an arc where the asteroid remains entirely within half a FoV from the targeted pointing, as this is a prerequisite to initialize the on-board relative navigation filter. Arcs 6, 9 and 10 in the sequence are identified as plausible candidates.

IV. GETTING MORE DARING: DETAILED CHARACTERIZATION PHASE

A. DCP Trajectory and Operational Characteristics

Following the ECP, a Payload Deployment Phase follows in which a set of slightly different arcs at 30 km distance at manoeuvre times is followed. In it, a similar navigation strategy to the one of ECP is applied. The goal of this phase is the dedicated support of the deployment and commissioning of the two cubesats ferried on-board Hera to the system and lasts from the 13th of January to the 3rd of February.

Following this phase, the focus shifts once again to further characterization of the system by entering a new phase, the Detailed Characterization Phase (DCP). Here, the spacecraft starts venturing even closer to the system, following a bowtie sequence of 4 arcs where the 4-day arcs venture down to pericentres around 11 km, while the manoeuvres happened at 22 km from the system and at a phase angle of 75 degrees. Before settling onto this motion, an intermediate manoeuvre at 26 km is used to avoid a too hastened descent, as a direct transfer was shown to compromise navigation performances. The phase spans 4 weeks from the 3rd of February to the 3rd of March. The trajectory is depicted in Fig. 10 and the evolution of distance, latitude and phase angles is given in Fig. 11.

B. Phase specific navigation assumptions

This phase is the first one in which landmarks navigation is baselined, along with the use of autonomous attitude guidance. Only Didymos landmarks are modelled, as previously described, and thus Dimorphos observations are treated as centroiding observable. Nevertheless, isolated Dimorphos observations are much less likely through this phase, as distance to the system is significantly reduced compared to previous phases and thus Didymos is quite likely to obstruct Dimorphos. The use of RCT thrusters is baselined for this phase, as they do not require a slew to and from a manoeuvre specific attitude and can be performed while in asteroid pointing attitude. The a-priori knowledge for Hera and the Didymos Barycentre state are based on results in the previous phase, although they are inflated to allow the filter to re-corelate the two solutions. The other parameters are lowered to the order of magnitude coming out of the ECP navigation analysis apart from the true longitude period. The values are listed in Table 7, along with values for the asteroid gravitational parameters and the initial state of the secondary's orbit.

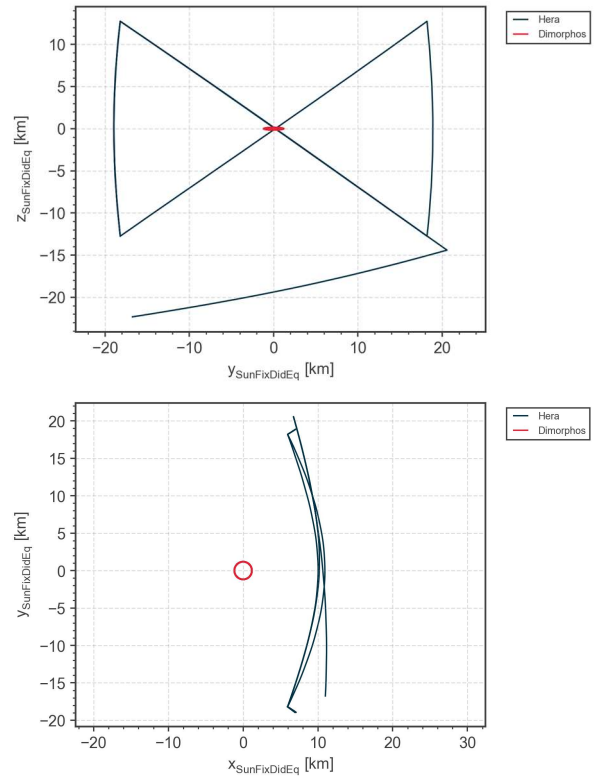


Fig. 10: DCP geometry around Didymos in Sun Fixed Didymos Equatorial plane. Top: Y-Z projection. Bottom: X-Y projection.

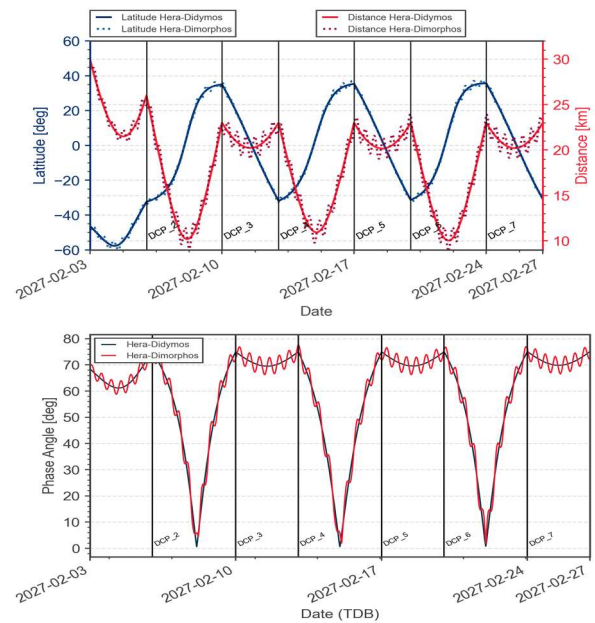


Fig. 11: DCP Geometrical Parameters. Top: Distance and Latitude. Bottom: Phase Angle.

The dispersion values are given in Table 8 and in this case they correspond in all cases to a-posteriori values from the ECP navigation analysis. The simulation begins at the start of PDP to allow the simulation to reach a steady state prior to the start of DCP.

Table 7: DCP Specific Solve-For Parameter Assumptions [1- σ]

Parameter	Value	Unit	Notes
Hera Position	5	km	Spherical
Hera Velocity	10	cm/s	Spherical
Didymos Barycentre Position	5	km	Spherical
Didymos Barycentre Velocity	5	cm/s	Spherical
Didymos GM	5	%	
Dimorphos GM	100	%	
True Longitude Period	50	s	
e_x, e_y	0.02	-	
\dot{i}_x, \dot{i}_y	0.002	-	
λ_0	2	deg	

Table 8: DCP Specific Navigation Analysis Dispersion Assumptions [1- σ]

Parameter	Value	Unit	Notes
Didymos-Hera Position	2	km	Spherical
Didymos-Hera Velocity	7	mm/s	Spherical
True Longitude Period	1	s	
e_x, e_y	0.05	-	
\dot{i}_x, \dot{i}_y	0.02	-	
λ_0	2	deg	

Finally, in this phase the concept of dogleg manoeuvres is used for the first time in the mission. This technique was previously used in Rosetta [13] and its purpose is to avoid low velocity excursions through the execution of the manoeuvre by splitting the manoeuvre in two legs. In this phase, the legs are chosen to avoid excursions below 0.4 safety margin over the instantaneous escape velocity. In the context of navigation, sometimes this is not possible because the correction of previous manoeuvre errors may demand that the spacecraft flies arcs with a safety margin below the one targeted or previous manoeuvre errors lead put the initial velocity of the manoeuvre below the targeted threshold. In these corner cases, the safety margin of the infringing velocity (either pre manoeuvre or post manoeuvre) is taken.

C. Navigation Analysis Results

Fig. 12 shows the evolution of instantaneous position knowledge between Didymos and Hera through the ECP phase. The position knowledge at manoeuvre times is significantly improved when compared to the ECP centroiding based approach thanks to the radial information obtained from the landmark observables and the higher precision of these observables on the plane of sky directions. Also in this phase, the spacecraft flies a very limited time close to the poor observation geometries seen in ECP which helps to avoid further degradation (see Fig. 13). Position knowledge at manoeuvre times ranges between highest eigenvalues of 150 to 180 m [1-sigma].

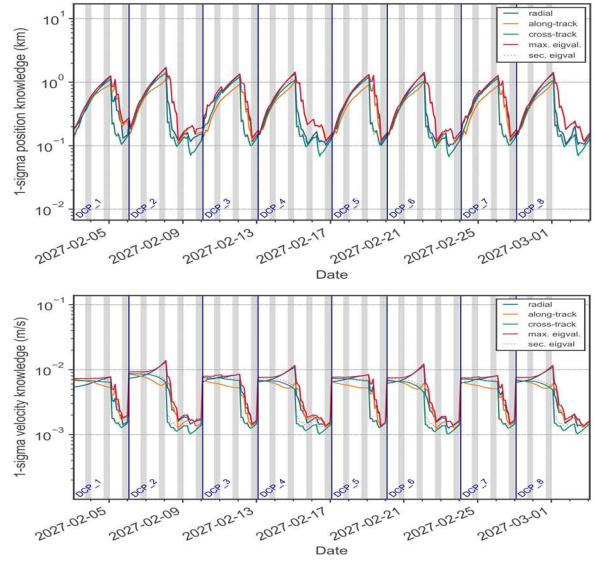


Fig. 12: DCP Knowledge Evolution. Vertical blue lines signal manoeuvre epochs and grey lines represent radiometric passes. Top: Position. Bottom: Velocity

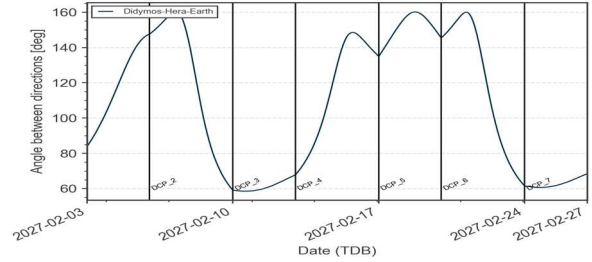


Fig. 13: Didymos – Hera – Earth angle through DCP

As Fig. 14 depicts, the observed landmark points are quickly estimated down to a higher eigenvalue on the order of meters and by the end of the phase the uncertainties for all observed landmarks are below 1 m. Some landmarks close to the poles are not well observed and landmarks on the norther hemisphere of the asteroid get more observability as the asteroid goes towards its northern hemisphere summer (this could be appreciated in Fig. 11).

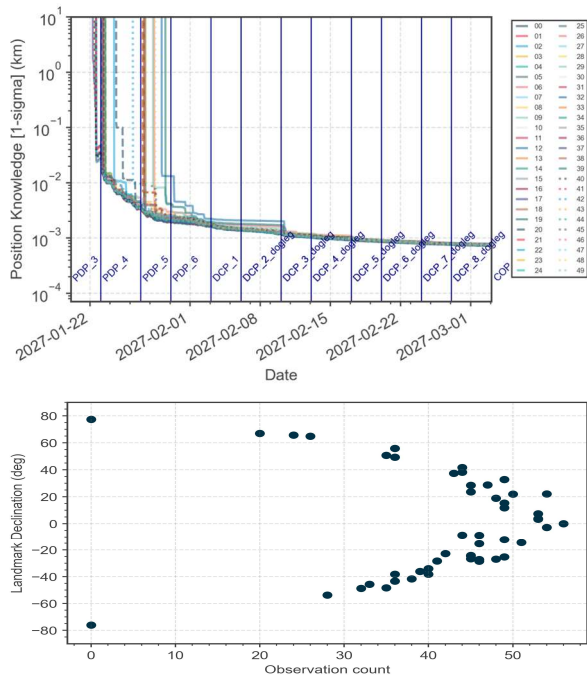


Fig. 14: Landmark estimation through the PDP and DCP phase. Top: Maximum Position eigenvalue for each landmark. Bottom: Distribution of landmarks in terms of observation count and declination

The estimation of the system further improves from the combination of landmark observables and the lower excursion flybys. The landmark observations on Didymos allow a good characterization of Dimorphos gravity effect on Didymos, bringing Dimorphos GM uncertainty down to 0.9% [1-sigma] while Didymos GM uncertainty is further lowered thanks to the lower pericentres to 0.3% [1-sigma]. Some J2 observability is present, with a-posteriori uncertainty at 0.4% [1-sigma] thanks to the independent observation of Didymos GM through lower flybys. Nevertheless, this cannot be considered that this is yet a satisfying determination of this spherical harmonics component, although it points to promising results for the phases following DCP, where Hera will go down to even lower pericentres. The relative motion between the two bodies is not significantly improved on the along track direction, as the performance of Dimorphos observables is bounded by the centroiding accuracy, although a slight improvement in the other two components is achieved down to 3 m [1-sigma] in both directions. As a result of this, the improvement in the orbit characterization is not too significant.

The position dispersion evolution for this phase oscillates between [1-sigma] maximum values of 1.7 km after the 3-day arcs at higher altitude to values up to 3 km following the 4-day arcs. This is a consequence of position dispersions around the lower pericentres, leading to significantly different departing hyperbolas between different orbits. Through pericentre the

dispersion is close to 15% [1-sigma] of the distance to the spacecraft. This higher pericentre dispersion puts into question the validity of the linear model used for this analysis, as the closer pericentre lead the spacecraft to regions with significantly more non-linear dynamics. Full dynamics propagations of dispersed samples after each manoeuvre (including doglegs) were undertaken to ensure that the trajectories are collision-risk free. The lowest pericentre observed within the 5000 samples was at 3.75 km to Didymos. Along with this, full dynamics propagations of samples in case of manoeuvre interruption were computed with only one case in one possible manoeuvre failure infringing below 2 km distance. All the samples were propagated for 14 days to show that none remained in a bounded orbit with the associated risk of impact in case of not recovering the spacecraft in time. No bounded orbit was found. Finally, a pointing error analysis was also performed to check that initialization conditions for the on-board attitude guidance were satisfactory. This was found to be the case for all manoeuvres.

V. CONCLUSION

Through this paper, a set of tools for small body navigation analyses, developed for Hera mission, has been presented along with a demonstration of its use for the ECP and DCP phases. This has allowed the examination and analysis of the operational concept for these phases, which has led to modifications to the trajectory and operational concept which should help ensure a successful navigation and exploration of the Didymos system.

VI. REFERENCES

- [1] P. Michel, M. Kueppers, H. Sierks, I. Carnelli, A. Cheng, K. Mellab, M. Granvik, A. Kestilä, T. Kohout, K. Muinonen, A. Näsilä, A. Penttilä, T. Tikka, P. Tortora, V. Ciarletti, A. Hérique, N. Murdoch, E. Asphaug, A. Rivkin, O. Barnouin A. Bagatin, P. Pravec, D. Richardson, S. Schwartz, K. Tsiganis, S. Ulamec and Ö. Karatekin, "European component of the AIDA mission to a binary asteroid: Characterization and interpretation of the impact of the DART mission," *Advances in Space Research*, vol. 62, no. 8, pp. 2261–2272, Oct. 2018, doi: 10.1016/j.asr.2017.12.020.
- [2] P. Michel, M. Küppers, A. Bagatin, B. Carry, S. Charnoz, J. Leon, A. Fitzsimmons, P. Gordo S. Green, A. Hérique, M. Juzi, Ö. Karatekin, T. Kohout, M. Lazzarin, N. Murdoch, T. Okada E. Palomba, P. Pravec, C. Snodgrass, P. Tortora K. Tsiganis, S. Ulamec, J. Vincent, K. Wünnemann, Y. Zhang, S. Raducan, E. Dotto, N. Chabot, A. Cheng, A. Rivkin, O. Barnouin, C. Ernst A. Stickle, D. Richardson, C. Thomas, M. Arakawa, H. Miyamoto, A. Nakamura, S.

- Sugita, M. Yoshikawa, P. Abell, E. Asphaug, R. Ballouz, W. Bottke, D. Lauretta, K. Walsh, P. Martino and I. Carnelli, “The ESA Hera Mission: Detailed Characterization of the DART Impact Outcome and of the Binary Asteroid (65803) Didymos,” *Planet Sci J*, vol. 3, no. 7, p. 160, Jul. 2022, doi: 10.3847/PSJ/ac6f52.
- [3] R. Pardo De Santayana and M. Lauer, “Optical Measurements for Rosetta Navigation near the Comet,” in *25th International Symposium on Space Flight Dynamics*, Munich, 2015.
- [4] B. Godard, F. Budnik, P. Muñoz, T. Morley, and V. Janarthanan, “Orbit Determination of Rosetta around Comet 67P/Churyumov-Gerasimenko,” in *25th International Symposium on Space Flight Dynamics*, Munich, 2015.
- [5] J. Miller, B. Williams, W. Bollman, R. Davis, C. Helfrich, D. Scheeres, S. Syimott, T. Wang D. Yeomans, J. Miller, B. Williams, W. Bollman, R. Davis, C. Helfrich, D. Scheeres, S. Syimott T. Wang and D. Yeomans , “Navigation of the Near Earth Asteroid Rendezvous Mission,” in *AAS/AIAA Spaceflight Mechanics Meeting*, Albuquerque, New Mexico, Feb. 1995.
- [6] T. Hashimoto, T. Kubota, I. Kawaguchi, M. Uo K. Shirakawa, T. Kominato and H. Morita, “Vision-based guidance, navigation, and control of Hayabusa spacecraft-Lessons learned from real operation”.
- [7] F. Terui, N. Ogawa, G. Ono, S. Yasuda, T. Masuda, K. Matsushima, T. Saiki and Y. Tsuda, “Guidance, navigation, and control of Hayabusa2 touchdown operations,” *Astrodynamics*, vol. 4, no. 4, pp. 393–409, 2020, doi: 10.1007/s42064-020-0086-5.
- [8] B. Williams, P. Antreasian, E. Carranza, C. Jackman, J. Leonard, D. Nelson, B. Page D. Stanbridge, D. Wibben, K. Williams, M. Moreau, K. Berry, K. Getzandanner, A. Liounis, A. Mashiku, D. Highsmith, B. Sutter and D. Lauretta, “OSIRIS-REx Flight Dynamics and Navigation Design,” *Space Sci Rev*, vol. 214, no. 4, p. 69, 2018, doi: 10.1007/s11214-018-0501-x.
- [9] The GODOT Team at ESA/ESOC, “GODOT (Generic Orbit Determination and Optimisation Toolkit).” ESA/ESOC, Darmstadt, 2024.
- [10] I. Acedo and P. Muñoz, “Trajectory Design and Navigation Analysis of Hera’s Rendezvous with the Didymos Asteroid System,” in *28th International Symposium on Space Flight Dynamics*, Beijing, Sep. 2022.
- [11] S. Naidu, L. Benner, M. Brozovic, M. Nolan S. Ostro, J. Margot, J. Giorgini, T. Hirabayashi, D. Scheeres. P. Pravec, P. Scheirich, C. Magri and J. Jao, “Radar observations and a physical model of binary near-Earth asteroid 65803 Didymos, target of the DART mission,” *Icarus*, vol. 348, p. 113777, Sep. 2020, doi: 10.1016/j.icarus.2020.113777.
- [12] H. Agrusa, I. Gkolias, K. Tsiganis, D. Richardson, A. Meyer, D. Scheeres, M. Čuk, S. Jacobson, P. Michel, Ö. Karatekin, A. Cheng, M. Hirabayashi, Y. Zhang, E. Fahnestock and A. Davis, “The excited spin state of Dimorphos resulting from the DART impact,” *Icarus*, vol. 370, p. 114624, Dec. 2021, doi: 10.1016/j.icarus.2021.114624.
- [13] P. Muñoz, F. Budnik, B. Godard, T. Morley, V. Companys, U. Herfort and C. Casas, “Preparations and Strategy for Navigation during Rosetta Comet Phase,” in *23rd International Symposium on Space Flight Dynamics*, Pasadena, 2012.